



This is a repository copy of *Mapping rail wear regimes and transitions* .

White Rose Research Online URL for this paper:
<http://eprints.whiterose.ac.uk/757/>

Article:

Lewis, R. and Olofsson, U. (2004) Mapping rail wear regimes and transitions. *Wear*, 257 (7-8). pp. 721-729. ISSN 0043-1648

<https://doi.org/10.1016/j.wear.2004.03.019>

Reuse

Unless indicated otherwise, fulltext items are protected by copyright with all rights reserved. The copyright exception in section 29 of the Copyright, Designs and Patents Act 1988 allows the making of a single copy solely for the purpose of non-commercial research or private study within the limits of fair dealing. The publisher or other rights-holder may allow further reproduction and re-use of this version - refer to the White Rose Research Online record for this item. Where records identify the publisher as the copyright holder, users can verify any specific terms of use on the publisher's website.

Takedown

If you consider content in White Rose Research Online to be in breach of UK law, please notify us by emailing eprints@whiterose.ac.uk including the URL of the record and the reason for the withdrawal request.



eprints@whiterose.ac.uk
<https://eprints.whiterose.ac.uk/>



White Rose
university consortium
Universities of Leeds, Sheffield & York

White Rose Consortium ePrints Repository

<http://eprints.whiterose.ac.uk/>

This is an author produced version of a paper published in **Wear**. This paper has been peer-reviewed but does not include the final publisher proof-corrections or journal pagination.

White Rose Repository URL for this paper:
<http://eprints.whiterose.ac.uk/archive/00000757/>

Citation for the published paper

Lewis, R. and Olofsson, U. (2004) *Mapping rail wear regimes and transitions*. *Wear*, 257 (7-8). pp. 721-729.

Citation for this paper

To refer to the repository paper, the following format may be used:

Lewis, R. and Olofsson, U. (2004) *Mapping rail wear regimes and transitions*. Author manuscript available at: [<http://eprints.whiterose.ac.uk/archive/00000757/>] [Accessed: *date*].

Published in final edited form as:

Lewis, R. and Olofsson, U. (2004) *Mapping rail wear regimes and transitions*. *Wear*, 257 (7-8). pp. 721-729.

MAPPING RAIL WEAR REGIMES AND TRANSITIONS

R. LEWIS^{a*}, U. OLOFSSON^b

^aDepartment of Mechanical Engineering, The University of Sheffield, Mappin Street,
Sheffield, S1 3JD, UK (email: roger.lewis@sheffield.ac.uk)

^bDepartment of Machine Design, KTH, SE 100 44 Stockholm, Sweden (email:
ulfo@md.kth.se)

* corresponding author

ABSTRACT

This paper outlines work carried out to produce maps of rail material wear coefficients taken from laboratory tests run on twin disc and pin-on-disc machines as well as those derived from measurements taken in the field. Wear regimes and transitions are identified using the maps and defined in terms of slip and contact pressure. Wear regimes are related to expected wheel/rail contact conditions and contact points (rail head/wheel tread and rail gauge/wheel flange). Surface morphologies are discussed and comparisons are made between field and laboratory data.

Keywords: Railway track, wear, wear transitions, wear mapping.

INTRODUCTION

In a wheel/rail contact, both rolling and sliding occur in the contact area. On straight track, the wheel tread is in contact with the rail head, but in curves the wheel flange may be in contact with the gauge corner of the rail. Flanging results in a large sliding motion in the contact. The contact area can be divided into stick (no slip) and slip regions. With increasing tangential load, the slip region increases and the stick region decreases, resulting in a rolling and sliding contact. When the tangential load reaches its saturation value the stick region disappears and the entire contact area is in a state of pure sliding. In curves, especially, there can be a large sliding component on the contact patch at the gauge corner of the rail head.

Due to this sliding, wear occurs in the contact under the poorly lubricated condition that is typical of wheel/rail contact. It has been observed during sliding wear that an increase of the severity of loading (normal load, sliding velocity, or surface temperature) leads at some stage to a sudden change in the wear rate (volume loss per sliding distance). The simplest classification of the types of wear exhibiting these different wear rates is *mild wear* and *severe wear*. Mild wear results in a smooth surface that often is smoother than the original surface, with minimal plastic deformation and oxide wear debris. Severe wear results in a rough surface that is usually rougher than the original surface, with extensive plastic deformation and flake-like metallic wear debris [1, 2]. Both mild wear and severe wear have been identified on track during field studies [3]. It was found that mild wear dominated at the rail head, but at the rail edge severe wear was clearly occurring. For pure sliding wear tests, such changes in wear mechanism result in jumps in wear rate when the severity of the contact conditions is increased (for example, by increasing the contact pressure, sliding velocity, or bulk material temperature) for any pair of materials [4]. By plotting wear maps of wear rate against contact pressure and sliding velocity, the various territories associated with different wear mechanisms and the transitions from mild to severe wear can be identified [4]. In

sliding wear maps produced by Lim and Ashby [4], up to seven wear regimens were apparent.

A different approach for considering wheel/rail wear data has been used by Bolton and Clayton [5]. This approach involves plotting wear rate in $\mu\text{g mass loss/m rolled/mm}^2$ contact area against $T\gamma/A$, where T is the tractive force (normal force multiplied by coefficient of friction), γ is the slip (percentage difference in surface speeds between the wheel and rail or test specimens) and A is the contact area. Three wear regimes were identified during twin disc testing of rail materials, *mild*, *severe* and *catastrophic*.

Likely wheel/rail contact conditions at a particular point on a track can be predicted using a number of different numerical techniques such as finite element analysis and multi-body dynamics simulations [6]. Once determined these can be used to identify the appropriate operating conditions for experimental studies of rail material wear. The aim of this work is to draw together available experimental data on rail wear, produce tools in the form of wear maps and relate the wear maps to a likely range of contact conditions for the wheel rail contact.

RAIL WEAR DATA

A large amount of data relating to rail material wear has been generated during experimental studies carried out over the last two decades (for example see [5, 7, 8, 9, 10]). Data from these studies and more recent investigations using current wheel and rail materials [3] were used in this work.

The data resulted from tests run on a range of equipment, from pin-on-disc and twin disc machines to full-scale wheel/rail test-rigs. Various material combinations and contact geometries were utilised as well as different test conditions (contact pressure and slip).

Presentation of data and completeness of data also varied. Chemical composition and hardness of the rail materials used in the tests, where available, is shown in Table 1.

WEAR TRANSITIONS

In order to present the data in a way that would allow a direct comparison, the approach first adopted by Bolton and Clayton [5] was used. As outlined above, this involves plotting wear rate against $T\gamma/A$. This approach has been used in much of the subsequent work on wheel and rail wear, but when different approaches had been taken, data was converted (if sufficient information about test conditions and specimen geometry was available) to enable it to be plotted using the parameters outlined above.

Three wear regimes have been identified during twin disc testing of rail materials [5, 11]. These were referred to as Type I (mild), Type II (severe) and Type III (catastrophic), as illustrated in Figure 1 using data for BS11 rail versus Class D tyre material taken from [5]. Each regime is defined in terms of wear rate, disc contact surface appearance, metallographic features of disc sections and wear debris. In the mild regime, wear appears to be dominated by surface oxidation [5, 11, 12], whereas in the severe and catastrophic regimes, it is dominated by surface cracking and material loss by spalling [5].

As can be seen in Figure 1, at the transition between each regime a distinct change in wear rate occurs. Mild to severe wear results from contact conditions most likely to occur in the wheel tread/rail head contact and severe to catastrophic wear in the wheel flange/rail gauge corner contact.

Similar trends in wear rate have been seen in subsequent twin disc testing, as shown in Figure 2. While it is clear that for each particular material combination the magnitude of wear and the location of the transitions between regimes are different the general trends are similar and

the same regimes exist. It is evident from the data presented in Figure 2 that wear rates are gradually reducing with the introduction of new materials, the wear rate for UIC60 900A rail steel being up to an order of magnitude lower than that of BS11.

A further wear mode, designated heavy wear, has also been identified within the severe regime [10]. The total wheel and rail wear rate data shown in Figure 3 (plotted against $p\gamma$, where p is the normal load) illustrates that this regime, characterised by a peak in the wear rate, exists for varying material combinations. It should be noted, however, that the significance of this peak is determined largely by the range of operating conditions under consideration. Obviously if the range extends into the catastrophic regime then the peak seen in the heavy regime is relatively small.

Work has shown that, within the severe wear regime (where wear rate is proportional to $T\gamma/A$), small-scale twin disc test results can be related to those from full-scale tests [13], as shown in Figure 4.

The full-scale test-rig results are in good agreement. Both show a linear relationship with a small difference in slope. It was thought that the difference in slope was due to underestimated slip values which would reduce values of the $T\gamma/A$ parameter. The spread of contact conditions for each flange contact represents a variation in the friction coefficient (accurate friction values could be determined for the tread contact so no spread occurred). The same applies to the field results, which were measured across the entire rail profile, where the rail is seeing a random distribution of wheel profiles. It is encouraging that, despite the mentioned deficiencies, the field and full-scale results are of the same order of magnitude as those for the small-scale tests.

The $T\gamma/A$ method of plotting data clearly allows for comparison of twin disc test data with full-scale test with field data, although very limited data is available from the latter.

WEAR COEFFICIENT MAPS

While using the $T\gamma/A$ method for plotting wear rate data enables wear transitions to be identified easily and comparisons of different material combinations to be made it does not help in fully understanding how the individual contributions of different parameters such as contact pressure and slip affect wear rate.

In order to allow a more complete analysis of the effect of individual parameters a mapping method was required for plotting wear data. It was decided that the most appropriate technique would be that developed by Lim and Ashby [4] for mapping sliding wear mechanisms.

Wear coefficients were calculated from the rail steel wear data using Archard's equation [14]:

$$K = \frac{Vh}{Ns} \quad (1)$$

where K is the wear coefficient, V is the wear volume, N is the normal load, s is the sliding distance and h is the material hardness.

Wear coefficients were then plotted against contact pressure and sliding speed in the contact. Two types of plots were constructed; contour maps and 3D point graphs. Obviously the accuracy of the contour map is limited by the amount of data available. The accompanying 3D graphs give an indication of where data is lacking on a particular map. Transitions based on those outlined above were marked on the contour plots.

Figure 5 illustrates data from twin disc testing using BS11 rail material versus Class D Tyre material (details in [5]). Data was available at high sliding velocities giving a more complete picture of wear likely under severe wheel/rail contact conditions. The upper plots show the full range of data available, while the lower plots focus on the mild to severe wear regimes where more data is available.

Figure 6 shows data from twin disc tests run at FAST (Facility for Accelerated Service Testing) using a standard carbon rail (details in [9]). Again the upper plots show the full range of data available, while the lower plots focus on the mild to severe wear regimes where more data is available.

The data for UIC60 900A rail versus R7 wheel material, shown in Figure 7, resulted from both twin disc and pin-on-disc tests (details in [3]). The pin-on-disc tests were carried out to simulate the higher sliding velocities encountered on tight curves. Such data was only available for this particular material combination. As can be seen a wear regime beyond catastrophic was apparent, where wear rates reduced to levels seen in the severe regime. A similar trend was observed in work in dry wear of steels [15] and also in ball bearing steels [4].

It is interesting to note that at low sliding velocities, the levels of the wear coefficients from the pin-on-disc tests and the two-roller tests are similar. The results show that the wear coefficient depends on the sliding velocity. The same tendency can be seen in the full-scale tests performed at Älvsjö test track [3]. The wear rate is higher at the rail edge (high sliding velocity) compared with wear rate at the rail head (low sliding velocity).

Wear magnitudes for UIC60 900A rail material versus R8T wheel material resulting from twin disc testing (shown in Figure 8) were similar to those seen with UIC60 900A versus R7. Not enough data was available to compile a meaningful contour map.

DISCUSSION

The aim of the work described was to produce tools in the form of maps of rail material wear data for identifying and displaying wear regimes and transitions. For this purpose wear data

was collected from small-scale and full-scale laboratory tests as well as measurements taken in the field.

Data for a range of wheel/rail material combinations has been presented using two methods; wear rate versus $T\gamma/A$ plots and wear maps showing wear coefficients versus contact pressure and sliding speed. These have highlighted that a number of rail steel wear regimes and transitions exist. The maps allow these to be analysed in terms of different contact parameters.

The $T\gamma/A$ plots have revealed that trends in wear rate, as the severity of the wheel/rail contact varies, are similar for a range of rail steels. They have also shown that over the last two decades wear rail steel wear rates have reduced by up to an order of magnitude. This in theory sounds positive, although it has been shown that decreasing wear may adversely affect crack growth in rails (wear would normally act to truncate cracks) leading to greater incidence of fatigue failures [16, 17].

The wear maps presented allow the contributions of sliding velocity and contact pressure to the wear rate to be isolated and give an understanding of where transitions occur between acceptable and more severe wear conditions. The wear maps also show that there is a clear difference in the wear rates for the wheel/rail material combinations studied in the severe wear regime, where rail steel wear rates have reduced by an order of magnitude over time. In the mild wear regime, however, it is hard to distinguish any difference in wear rate between the different combinations.

Relating expected pressure and slip in the wheel/rail contact at certain points on a track route, particularly low radius curves, to the amount of wear likely to occur under such conditions, is very important. It can help in determining:

- more efficient maintenance schedules on particular routes

- where different track profiles may be needed to reduce the severity of the wheel/rail contact
- where application of lubrication may be necessary to reduce wear problems.
- improving data input to simulation techniques used to predict rail profile change.

The data used in constructing the wear maps, however, is somewhat limited, which restricts their usefulness. The maps really represent a starting point and while initially they may only be useful in focussing areas in which to carry out further testing will nonetheless be very useful. It has been noted that the challenge is to extend maps such as these from the basis of empirical observation to that of theory calibrated against experiment [4].

Small Scale Laboratory Data versus Field Data

The small scale laboratory data shows a large increase in the wear rate when transferring from the mild to the catastrophic wear regime. Both mild wear and a more severe wear regime have been identified on track during field tests [3]. Pin-on-disc tests have been carried out using test specimens cut out and manufactured from wheel pieces from the rolling stock and rail sections that had been in use on the Älvsjö test tracks (see [3] for details). In this way full-scale field data can be compared with pin-on-disc data from exactly the same material batches. The field tests were evaluated using Archard's equation [14] (Equation 1). The material hardness, H , is the measured rail hardness and the sliding distance, s , was determined from the number of bogies passing over the section of test track using the assumption that for the leading bogie the first wheelset was in contact at the high rail gauge corner and the second wheelset was in contact with the high rail head. The normal loads were determined from train dynamic simulations (see [18]). Figure 9 shows the Archard wear coefficients for field data from the Älvsjö test track compared with those for pin-on-disc

tests. It can be seen that the ranking of the wear rates agrees reasonably well between full-scale field test and laboratory tests. In the full-scale tests the wear measured at the rail edge was six times higher than that at the rail head. In the pin-on-disc tests the wear rate in the catastrophic regime was four times higher than in the mild regime. The wear rate for the full-scale field tests are lower than the pin-on-disc results. This is probably due to the difference in environmental control between the two tests. In the full-scale field tests natural lubrication as high humidity and biological material will influence the wear rate. In contrast, the pin-on-disc tests were run in a controlled environment with constant temperature and humidity and the tests specimens were ultrasonically washed before testing.

Wear Regimes and Mechanisms

It is clear, from studying the literature, that while rail steel wear regimes have been defined well in terms of wear rate, metallographic features and wear debris, it is not understood what mechanisms are leading to the changes in wear rate that occur.

It has been postulated that temperature may play a role in the wear transitions [19]. In recent work on wear of R8T wheel steel [20] a quantitative analysis has been used to relate the wear transition between severe and catastrophic wear to the temperature in the contact. Temperatures calculated at the contact conditions seen around this transition were in the region at which a drop in yield strength of the wheel material occurs.

Calculations were carried out to determine temperatures in the pin-on-disc contact and twin disc contact for the UIC60 900A rail steel versus R7 wheel steel tests (see Figure 7 for wear rates). The pin-on-disc contact temperature calculations were carried out using the method outlined by Lim and Ashby [4] and for the twin disc contact calculations the approach set out by Lewis et al. [20] was used. The results, shown in Figure 10, indicate that the transition

from severe to catastrophic wear occurs between 200°C and 300°C. These temperatures correspond with those causing a drop in the yield strength of carbon manganese steels similar to rail steels [21].

Comparison of the pin-on-disc tests and twin disc tests at low load and sliding velocity indicate that similar temperatures were apparent, which would explain the similarity in wear rates observed.

Results from twin disc tests carried out using UIC60 900A rail steel and R8T wheel steel are shown in Figure 11. These also show the wear transition occurring at around 200°C.

Wear versus Wheel/Rail Contact Conditions

In previous work on wear of rail steel no attempt has been made to correlate wear data to wheel/rail contact conditions. The wheel/rail contact conditions illustrated in Figure 12 resulted from a study using GENSYS train dynamic modelling software [6]. As can be seen a clear difference exists between the rail head/wheel tread and the rail gauge/wheel flange contacts. The two points highlighted show results from Medyna simulations of the Älvsjö test track [22] for the first and second wheelsets, which provide a measure of corroboration.

To study how the wear regimes identified above fit in with the wheel/rail contact conditions shown in Figure 12 the wear map of UIC60 900A rail steel versus R7 wheel steel has been overlaid, as shown in Figure 13. This indicates that the rail head/wheel tread contact will experience mild to severe wear and the rail gauge/wheel flange contact will experience severe to catastrophic wear. This backs up previous suppositions regarding the wear regimes that the rail head/wheel tread and rail gauge/wheel flange contacts fall into. Surface topography measurements at the Älvsjö test track [3] identified mild wear as the dominating mechanism at the rail head, but at the rail edge a more severe or catastrophic wear was occurring. For the

pin-on-disc tests, a change in surface appearance was also noted. For the tests at low sliding velocity a smooth surface was observed, but at higher sliding speeds, the surface had a rougher appearance similar to that found at the rail edge for the full-scale tests.

Figure 14 shows the wear data points collected for various rail materials in terms of the contact conditions. It can be seen that there is a large amount of wear test data for conditions typical of a rail head/wheel tread contact, but very little for the rail gauge/wheel flange contact. This clearly identifies an area that needs to be addressed in future research. Especially as axle loads are increasing and rolling stock is being used on track with low radius curves as well as the high radius curves on high speed lines, which means it is likely that the severity of the wheel/rail contact conditions will rise.

Increasing the wear data available will also improve the accuracy and applicability of the wear maps.

CONCLUSIONS

- In this paper available experimental data on rail wear have been collected and presented in form of wear maps. Up to five wear regimes and transitions have been identified.
- Rail steel wear rates have reduced by up to an order of magnitude for the severe wear regime in the last 20 years. This is probably due to increased durability of rail materials and changes in wheel materials. For the mild wear regime it is hard to detect any change for the wheel/rail material combinations studied.
- By combining the wear maps with multi-body simulations the likely wear rates and wear regimes for rail head/wheel tread and rail gauge/wheel flange contacts can be predicted.

- The ranking of the wear rates agrees reasonably well between full-scale field test and laboratory tests. In the full-scale tests the wear measured at the rail edge was six times higher than that at the rail head. In the pin-on-disc tests the wear rate in the catastrophic regime was four times higher than in the mild regime.
- Temperature calculations for the twin disc and pin-on-disc contacts showed that the large increase in wear rates seen at the second wear transition (severe to catastrophic) may result from a thermally induced reduction in yield strength and other material properties.
- Gaps have been identified in current knowledge both in terms of rail steel wear data and wear mechanisms that provide a focus for new research in this area.

ACKNOWLEDGEMENTS

The authors would like to acknowledge the Royal Academy of Engineering (UK) for the provision of an International Travel Grant allowing Dr Lewis to visit KTH and collaborate with Dr Olofsson on this work.

REFERENCES

- [1] Williams, J.A., 1999, "Wear Modelling: Analytical, Computing and Mapping: A Continuum Mechanics Approach", *Wear*, 1999, Vol. 225–229, pp1–17.
- [2] Archard, J.F. and Hirst, W. 1956, "Wear of Metals Under Unlubricated Conditions" *Proceedings of The Royal Society*, London, Part A, 236, 3–55
- [3] Olofsson, U., Telliskivi, T., 2003, "Wear, Friction and Plastic Deformation of Two Rail Steels - Full-Scale Test and Laboratory Study", *Wear*, Vol. 254, pp80-93.

- [4] Lim, S.C., Ashby, M.F., 1987, "Wear Mechanism Maps", *Acta Metallica*, Vol. 35, pp1-24.
- [5] Bolton, P.J., Clayton, P., 1984, "Rolling-Siding Wear Damage in Rail and Tyre Steels", *Wear*, Vol. 93, pp145-165.
- [6] Jendel, T., 2000, "Prediction of Wheel Profile Wear – Methodology and Verification", Licentiate Thesis, TRITA-FKT 2000:9, Royal Institute of Technology, Stockholm, Sweden.
- [7] Clayton, P., 1996, "Tribological Aspects of Wheel-Rail Contact: A Review of Recent Experimental Results", *Wear*, Vol. 191, pp170-183.
- [8] Krause, H., Poll, G., 1986, "Wear of Wheel-Rail Surfaces", *Wear* Vol. 113, pp103-22.
- [9] Danks, D., Clayton, P., 1987, "Comparison of the Wear Process for Eutectoid Rail Steels: Field and Laboratory Tests", *Wear*, Vol. 120, pp233-250.
- [10] Zakharov, S., Komarovskiy, I., Zharov, I., 1998, "Wheel Flange/Rail Head Wear Simulation", *Wear*, Vol. 215, pp18-24.
- [11] Beagley, T.M., 1976, "Severe Wear of Rolling Sliding Contacts", *Wear*, Vol. 36, pp317-335.
- [12] Deters, L., Proksch, M., 2003, "Friction and wear of rail and wheel material", *Proceedings of CM2003, 6th International Conference on Contact Mechanics and Wear of Rail/Wheel Systems*, Vol. 1, pp175-181.
- [13] McEwen, I.J., Harvey, R.F., 1985, "Full-Scale Wheel-on-Rail Wear Testing: Comparisons with Service Wear and a Developing Theoretical Predictive Method", *Lubrication Engineering*, Vol. 41, No. 2, pp80-88.

- [14] Archard, J.F., 1953, "Contact and Rubbing of Flat Surfaces", *Journal of Applied Physics*, Vol. 24, pp981-988.
- [15] Welsh, N.C., 1965, "The Dry Wear of Steels, I, The General Pattern of Behaviour, II, Interpretation and Special Features", *Proceedings of the Royal Society Series A*, Vol. 257, pp31-70.
- [16] Olofsson, U. and Nilsson, R., 2002, "Surface Cracks and Wear of Rail: A Full-Scale Test and Laboratory Study", *Proceedings of the IMechE, Part F, Journal of Rail and Rapid Transit*, Vol. 216, pp249-264.
- [17] Kapoor, A., Fletcher, D.I., Franklin, F.J., 2003, "The Role of Wear in Enhancing Rail Life", *Proceedings of the 29th Leeds-Lyon Symposium on Tribology*, Elsevier Tribology Series No. 41, pp331-340.
- [18] Telliskivi, T. Olofsson, U., 2001 "Contact Mechanics Analysis of Measured Wheel-Rail Profiles Using the Finite Element Method", *Proceedings of the IMechE, Part F Journal of Rail and Rapid Transit*, Vol 215, pp 65-72.
- [19] Krause, H., Poll, G., 1986, "Wear of Wheel-Rail Surface", *Wear*, Vol. 113, pp103-122.
- [20] Lewis, R., Dwyer-Joyce, R.S., 2004, "Wear Mechanisms and Transitions in Railway Wheel Steels", submitted to *Proceedings of the IMechE, Part J Journal of Engineering Tribology*.
- [21] British Steel Makers Creep Committee, 1973, *BSCC High Temperature Data*, The Iron and Steel Institute for the BSCC, London.
- [22] Knothe, K., Theiler, A., Guney, S., 1999, "Investigation of Contact Stresses on the Wheel/Rail-System at Steady State Curving", *Proceedings of the 16th IAVSD Conference*, Pretoria, South Africa, 30 August - 3 September.

Figure Captions

Figure 1	Wear Regimes Identified during Twin Disc Testing of BS11 Rail Material versus Class D Tyre Material [5]
Figure 2	Wear Rates Resulting from Twin Disc Testing for a Number of Different Material Combinations
Figure 3	Total Wheel and Rail Wear Rate in the Heavy Wear Regime
Figure 4	Comparison of Rail Wear Data from Small and Full-Scale Tests and the Field [11]
Figure 5	Wear Coefficient Maps for BS11 Rail Material versus Class D Tyre Material (data from [5])
Figure 6	Wear Coefficient Maps for Standard Carbon Rail Material and an Unspecified Wheel Material (data from [9])
Figure 7	Wear Coefficient Maps for UIC60 900A Rail Material versus R7 Wheel Material (data from [3])
Figure 8	Wear Coefficient Map for UIC60 900A Rail Material versus R8T Wheel Material
Figure 9	Field Data from the Älsvjö Test Track [3] Compared with Pin-on-Disc Data from the same Material Batches (UIC60 900A rail material versus R7 wheel material).
Figure 10	Contact Temperatures and Wear Coefficients for Twin Disc Tests and Pin-on-Disc Tests for UIC60 900A Rail Material versus R7 Wheel Material (lower graph is a magnification of upper graph)
Figure 11	Twin Disc Contact Temperatures and Wear Coefficients for UIC60 900A Rail Material versus R8T Wheel Material
Figure 12	Wheel/Rail Contact Conditions on the Stockholm Local Railway Network Derived from GENSYS Simulations [6] (also shown are results from Medyna simulations of the Älsvjö test track [18] for the first and second wheelsets)
Figure 13	UIC60 900A Rail Steel Wear Map Plotted Over Wheel/Rail Contact Conditions Derived from GENSYS Simulations [6]
Figure 14	Available Rail Steel Wear Data Plotted Over Typical Wheel/Rail Contact Conditions
Table 1	Material Specifications

Figure 1

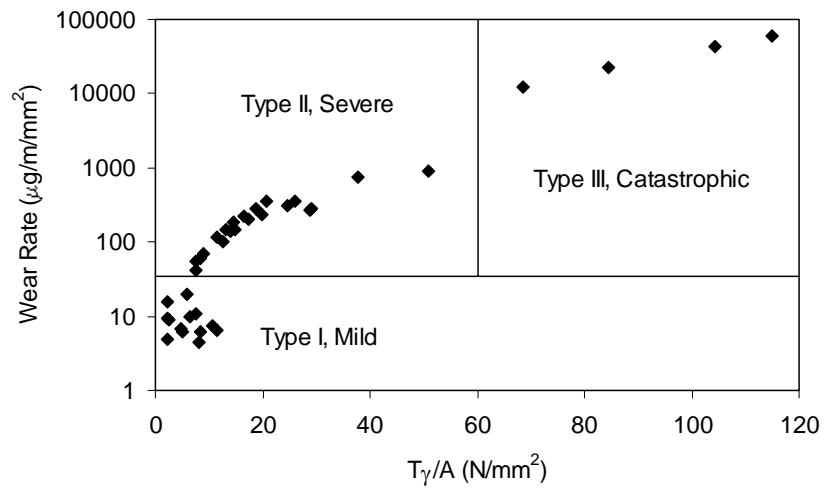


Figure 2

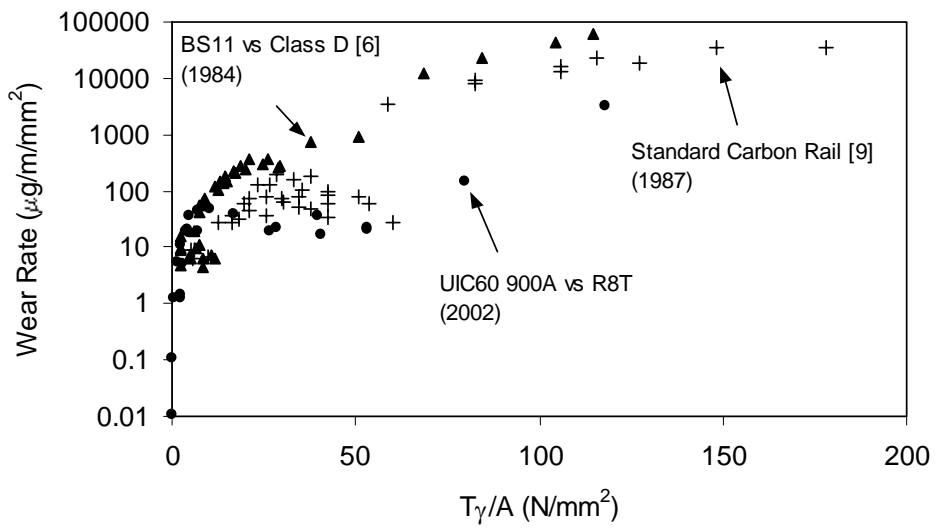


Figure 3

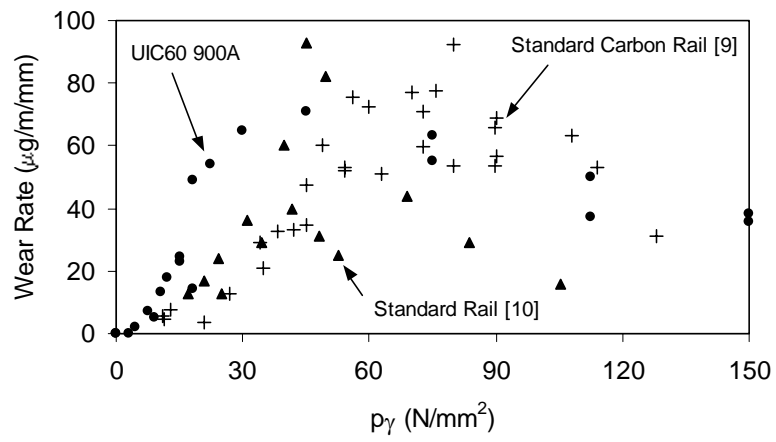


Figure 4

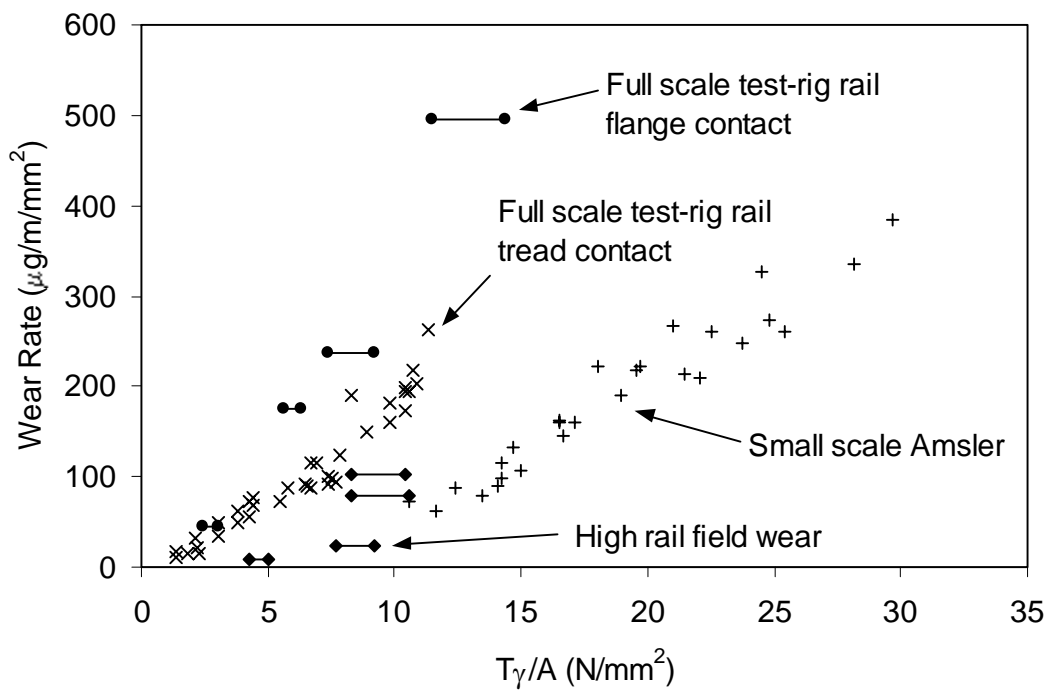


Figure 5

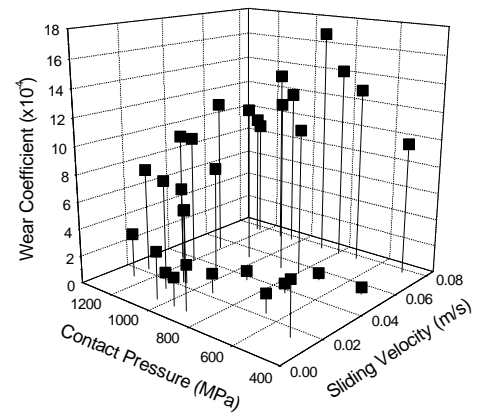
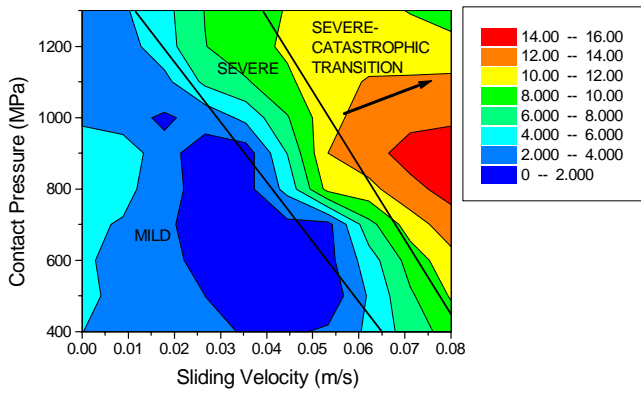
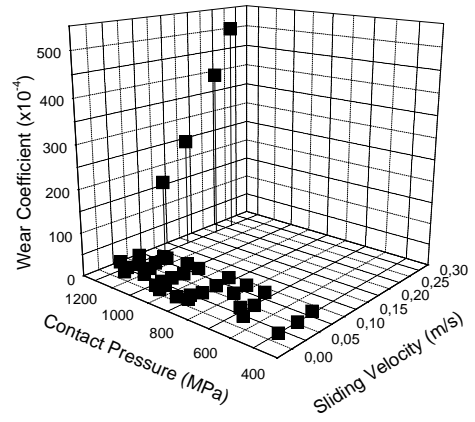
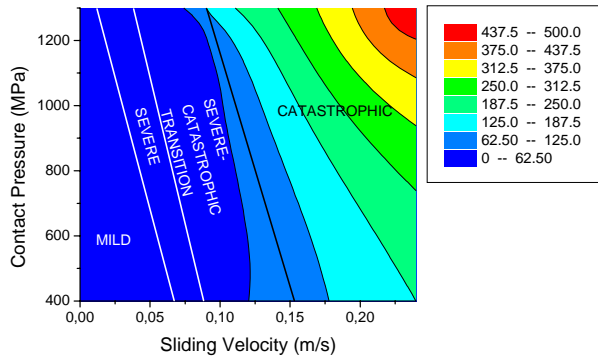


Figure 6

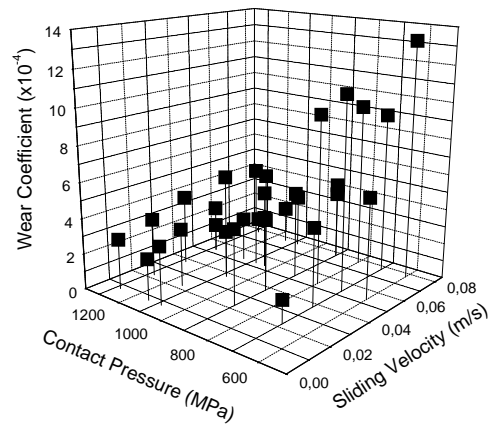
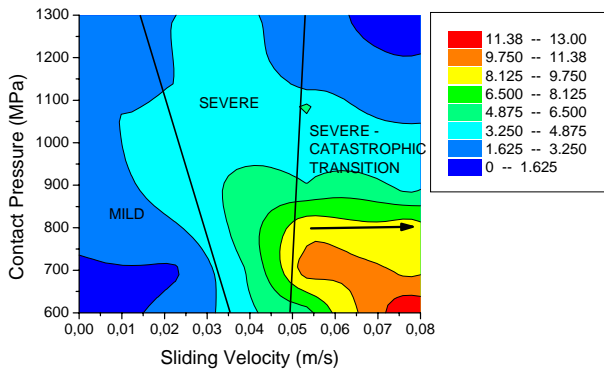
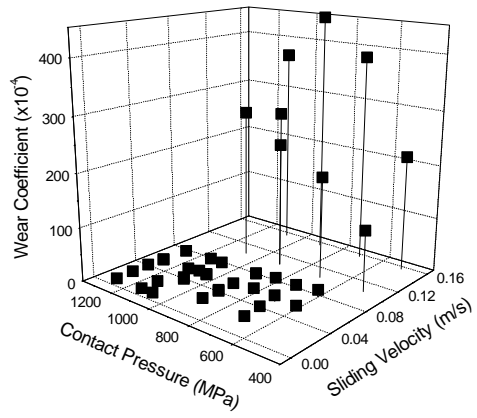
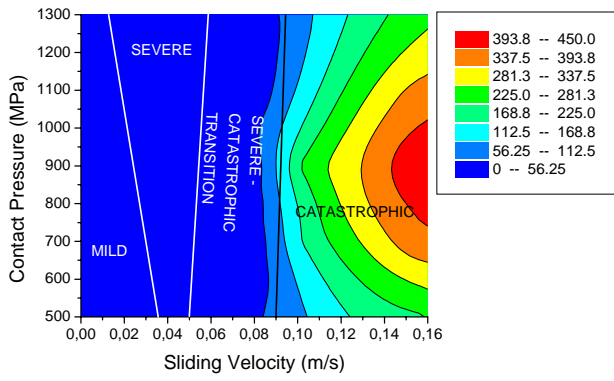


Figure 7

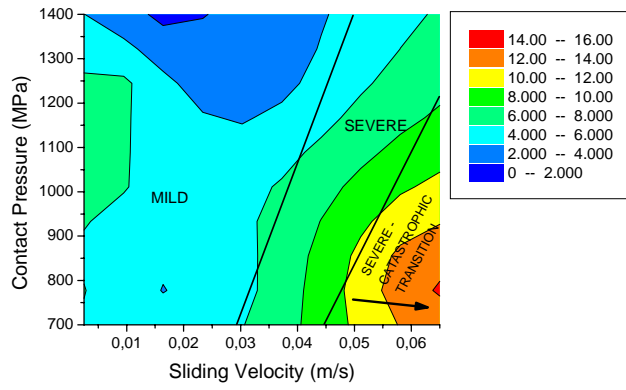
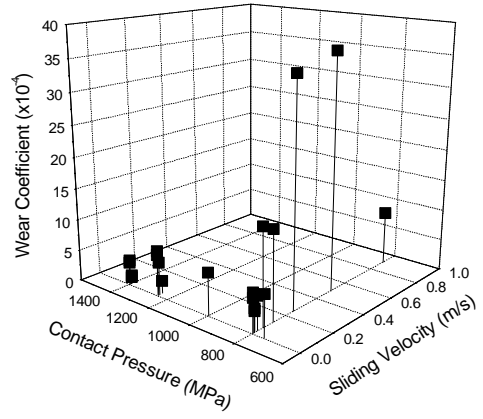
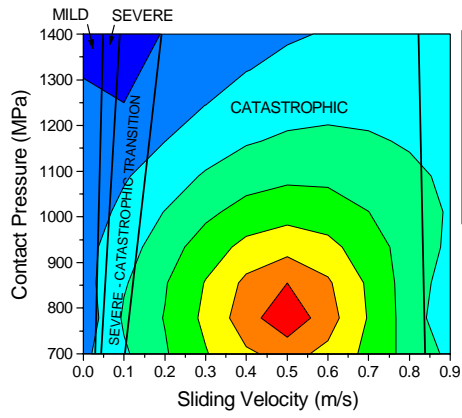


Figure 8

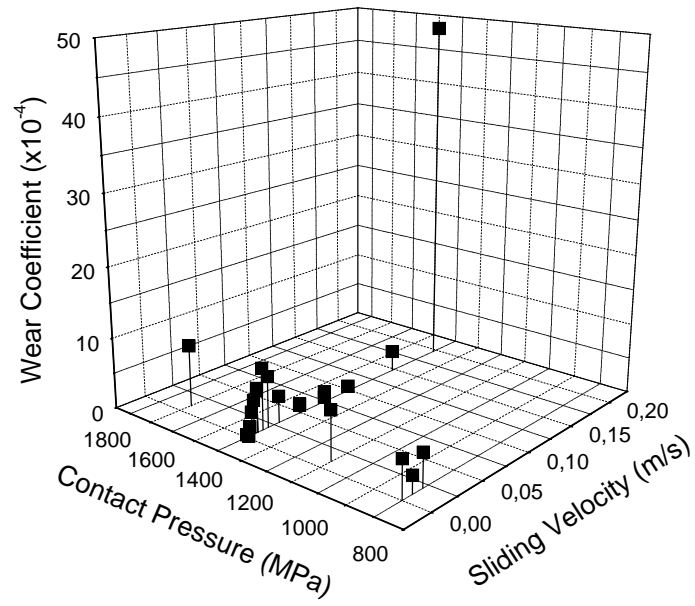


Figure 9

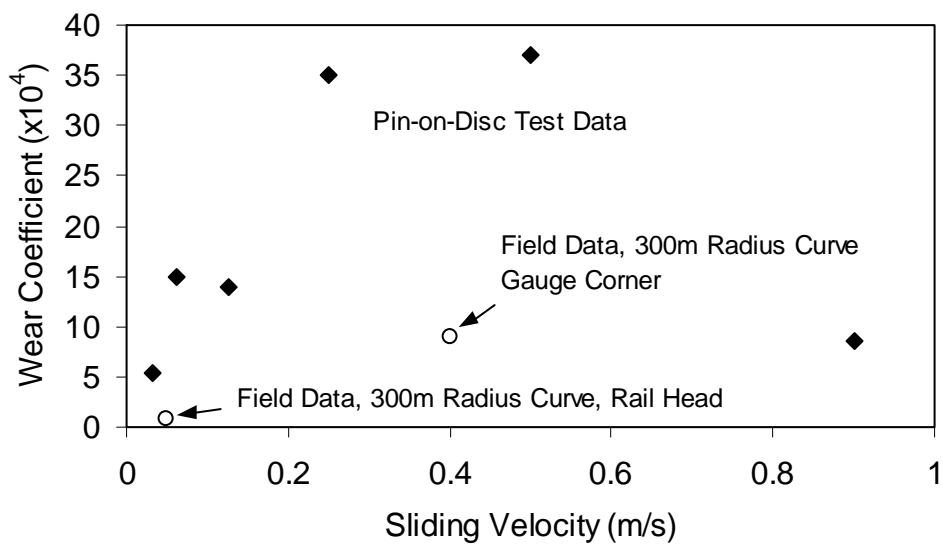


Figure 10

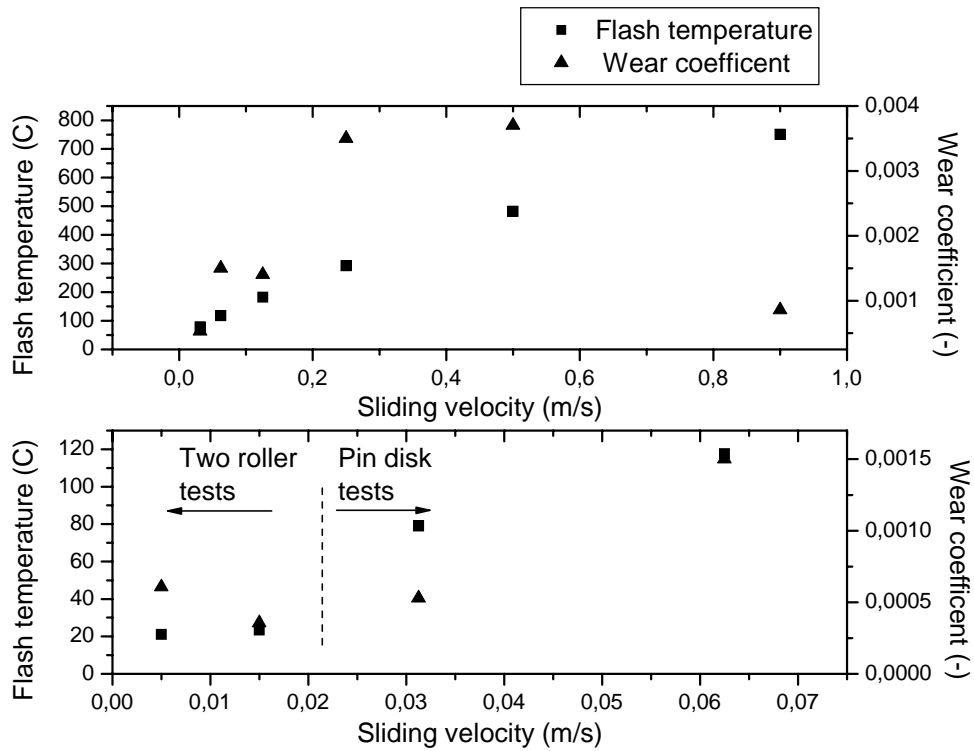


Figure 11

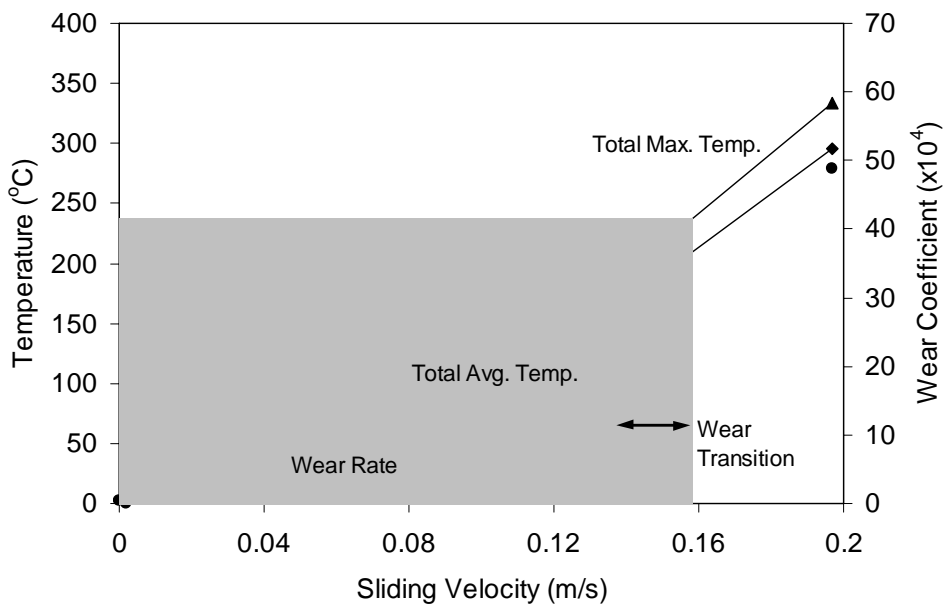


Figure 12

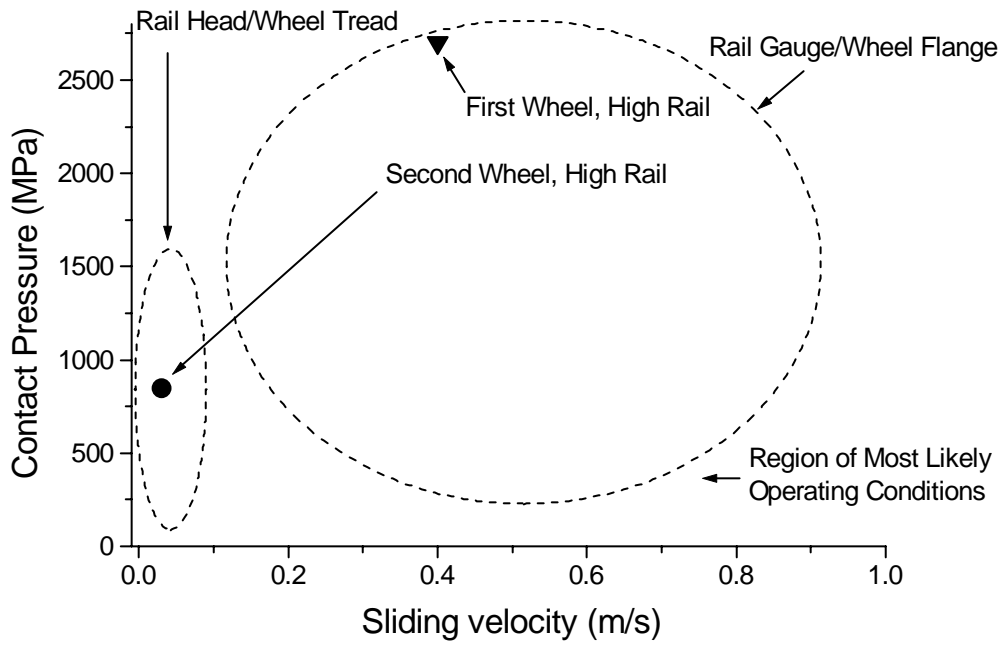


Figure 13

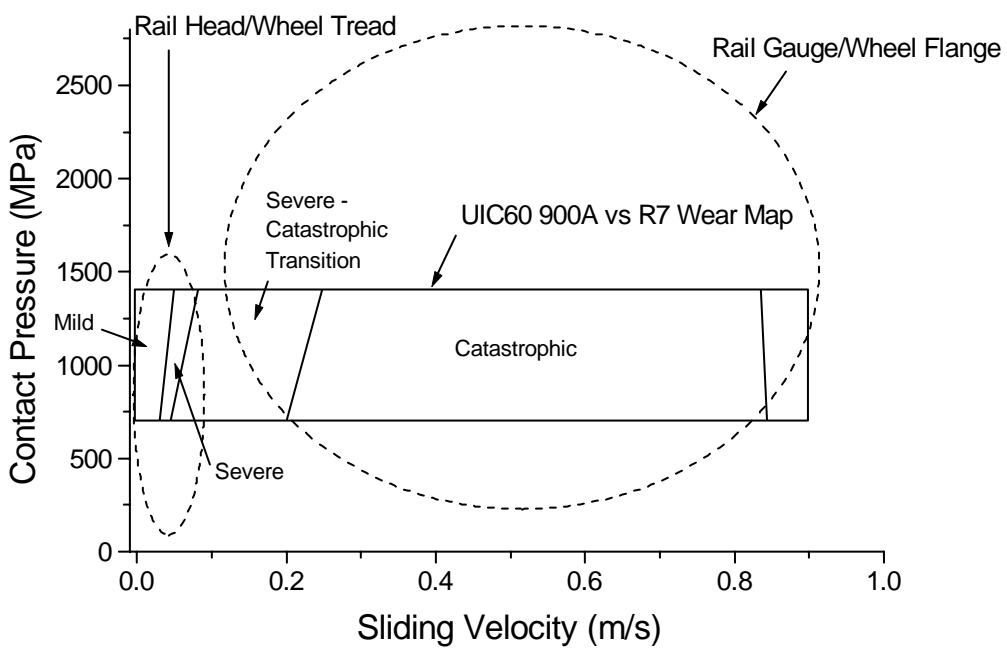


Figure 14

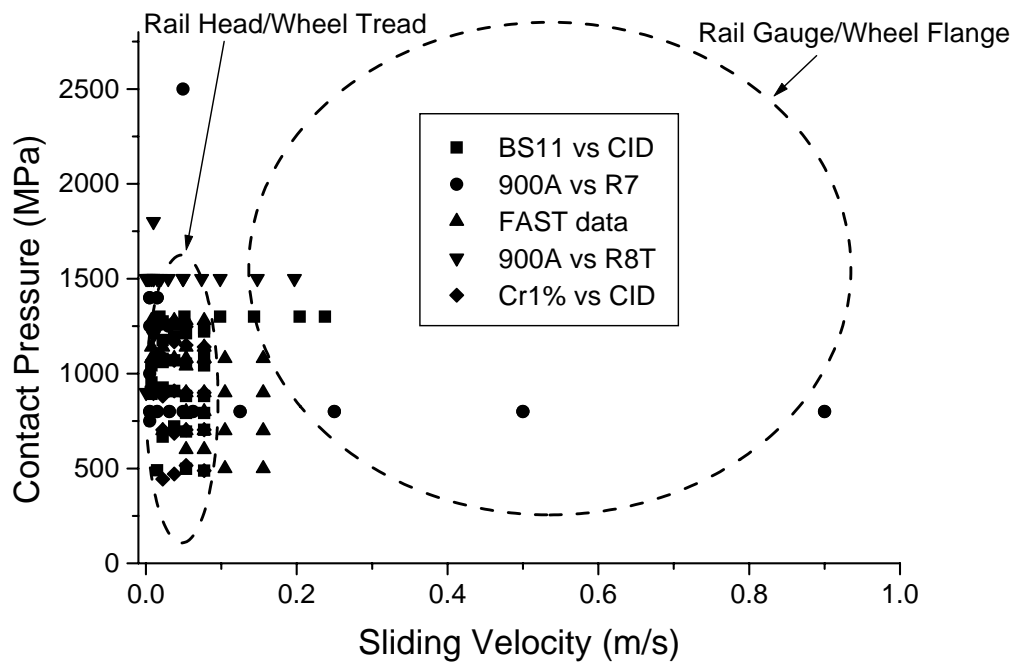


Table 1

Reference	Material	Chemical Composition (wt. %)												Hardness (GPa)
		C	Mg	Si	Mn	S	F	P	Ni	Cr	Mo	Cu	Sn	
[9]	Standard Carbon Rail	0.75		0.25	0.98	0.03		0.4	0.09	0.02	0.01			2.42
	Wheel	0.77		0.33	0.66	0.04		0.03	0.08	0.08	0.04			2.42
[10]	Rail	0.75	1.05	0.22		0.023	0.027							2.90
	Wheel	0.62	0.63	0.29		0.021	0.023							2.90
[3]	UIC60 900A Rail	0.6- 0.8		0.15- 0.5	0.8- 1.3									2.65
	UCI60 1100 Rail	0.63- 0.78		0.3- 0.8	0.85- 1.3			0.04						3.23
	R7 Wheel	0.52		0.4	0.8			0.035	0.3	0.3				2.75
[5]	BS11 Rail	0.53		0.26	1.07	0.02		0.021	0.02	0.02	0.01			2.45
	1% Chrome Rail	0.70		0.14	1.18	0.029		0.024	0.01	1.08	0.01			3.23
	Class D Tyre	0.65		0.24	0.71	0.046		0.026	0.15	0.18	0.03	0.26	0.031	